AMSE JOURNALS-AMSE IIETA publication-2017-Series: Modelling C; Vol. 78; N°1; pp 100-115
Submitted Jan. 2017; Revised March 15, 2017, Accepted April 15, 2017

A Theoretical Study of Heat and Mass Transfer in Forced Convective Chemically Reacting Radiating MHD Flow through saturated Porous Medium over Fixed Horizontal Channel

Pooja Sharma[*], Ruchi Saboo[**]

[*,**]Department of Mathematics & Statistics, Manipal University Jaipur, Jaipur, India
([*]pooja_2383@yahoo.co.in, [**]ruchipsaboo@gmail.com)

Abstract

In the present study; the effect of chemical reaction, viscous dissipation are considered in the steady forced convective chemically reactive radiating MHD flow through the horizontal channel with joule heating. The channel is saturated with uniform porous medium and having a insulated, impermeable bottom wall. The governing equations for velocity, temperature and concentration field are obtained and solved. The effect of various physical paramteres over these fluids are considred and showed through graphs. The expression for mean velocity, mean temperature and mean concentration are also presented. The numerical values of Nusselt number, skin-friction & Sherwood number are discussed through the table. It was concluded that; for high depth porous medium channel the flud mean temperature and species mean concentration both rise high. Fluid flow can be made fast in this geometrical fluid flow by increasing the depth of the porous medium

Keywords

Mass transfer, Thermal radiation, Chemical reaction, Heat source, MHD.

1. Introduction

The behaviour of synchronized heat and mass transfer in the presence of magnetic field has fascinated numerous investigators due to its several kinds of practices in engineering and scinces such as polymer solutions, biomedicine, plasma astronomy, geological physics, processing of food, oceanlogy and in many fluid flow problems. In recent years, different fluid flows in porous medium has been considered by many of the researchers in different geometries in the presence of various physical condition. Kuznestov et al.[1] studied the mass exchange of the glass and the

effect of thermal insulation on that. Abdullah[2] proposed the study of composite materials in place of thermal insulation. The mixed convection flow is discussed by Reddy et al.[3] in the presene of thermal diffusion and chemical reaction. Yao et al.[4] studied the heat transfer in porous copper foam heat pipes. Zeng et al.[5] considered the small cavity to examine the heat transfer and characteristics of natural convection. Magnetic field effect with heat and mass transfer on the partial slip flow through vertical insulated porous plate was investigated by Baoku[6]. In view of that Thakur et al.[7] extended the study to examinethe MHD flow of micropolar fluid with variable viscosity in the same geometry. MHD natural convection flow was also discussed by Jha et al.[8] in the vertical parallel plate microchannel. Umavathi et al.[9] inspected the oscillatory flow with heat transfer in a porous medium channel. Bakkas et al.[10] also considered the same geometry with rectangular blocks relasing heat flux with natural convection heat transfer. The same study in porous media square cavity covered with cold walls was probed by Duan et al.[11]. Joule heating and magnetic field effects in combined convection through a lid driven cavity in the presence of rolled bottom surface was investigated by Pravin et al.[12]. Liuw et al.[13] studied the secondary flow and heat transfer in horizontal channels heated from below. Makinde et al.[14] also considered the channel filled with soaked porous medium for temporal stability analysis of hydromagnetic flow. Mounuddin et al.[15] studied the steady fluid flow through channel saturated with porous medium with impermeable and thermally insulated bottom. Raju [16] extended their study with viscous dissipation and joule heating in the presence of transvese magnetic field. Recently Zeghbid et al.[17] deliberated the mixed convection in lid-driven cavities. Heat and mass transfer study between hot and cold vertex cores inside a vertex tube was considered by Rafiee et al.[18]. Niche et al.[19] investigated the doufour and soret effects in unsteady double diffusive natural convection. Chemically reacting MHD visco-elastic fluid flow with thermal diffusion was studied by popoola et al.[20]. MHD flow through rotating channel with mass transfer was explored by Ahmed et al.[21].

Motivated by above citied work we have made an attempt to extand the study of Raju et al.[16] with mass transfer effects in the presence of heat source and with impact of thermal radiation.

In the present study the heat and mass transfer in two dimensional chemically reactive steady MHD forced convective flow of a viscous fluid through a horizontal channel soaked with porous medium and fixed impermeable thermally insulated bottom surface in the presence of heat source and thermal radiation.

2. Mathematical formulation

We consider a chemically reactive steady flow of a viscous incompressible, electrically conducting, forced convective flow through a soaked porous medium of depth H with impermeable and thermally insulated bottom in the presence of transverse magnetic field, heat source and thermal radiation. The schematic diagram of the flow geometry is given in fig.1.

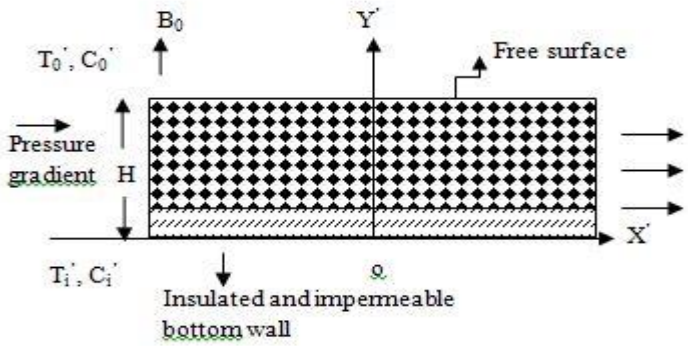

Fig.1. Flow configuration

According to figure 1, we consider a rectangular co-ordinate system, with the reference of that the origin is considered on the bottom surface and X'-axis is along the flow direction. The height H of the porous medium is assumed in the Y'-axis direction. Therefore the bottom is considered as Y'=0 and the free surface is considered as Y'=H. The uniform magnetic field is working in the transverse direction of the fluid flow. The upper side of the porous medium is supposed as free surface which is open to environment of constant temperature T_1.

The following assumptions are supposed in the considered physical problem:

(1)The induced magnetic field is negligible in comparison of the functional magnetic field due to the small magnetic Reynolds number.

(2)The fluid is considered as electrically conducting fluid. The positive negative charged particles are approximately equivalent in a small finite volume of the fluid. Therefore the total additional charge mass and executed electric field strength is expected to be nil.

(3)The fluid flow is caused due to uniform horizontal pressure gradient at the left open side of the channel along the bottom line. The fluid velocity is U' in the X'-direction.

(4)The generalized Darcy's law suggested by Yamamoto & Iwamura[22] is anticipated in the momentum equation, in which classical Darcy force is considered to be associated with convective acceleration and Newtonian- viscous stresses.

Under the above assumptions, the governing equations of the fluid flow are specified as below:

$$-\frac{\partial P}{\partial X^{'}}+\mu\frac{d^2U^{'}}{dY^{'2}}-\mu\frac{U^{'}}{K^{'}}-\sigma B_0^2U^{'}+g\beta(C_1^{'}-C_0^{'})=0 \tag{1}$$

$$\rho CpU^{'}\frac{\partial T^{'}}{\partial X^{'}}=\kappa\frac{d^2T^{'}}{dY^{'2}}+\mu\left(\frac{dU^{'}}{dY^{'}}\right)^2+\sigma B_0^2U^{'2}+\frac{Q_0}{\rho Cp}\left(T_1^{'}-T_0^{'}\right)-\frac{dq_r^{'}}{dY^{'}}=0 \tag{2}$$

$$\frac{d^2C^{'}}{dY^{'2}}-k_l\left(C_1^{'}-C_0^{'}\right)=0 \tag{3}$$

It is assumed that the medium is optically thin with relatively low density. Following Cogely[23] equilibrium model, the radiative heat flux term is given by

$$\frac{\partial q_r^{'}}{\partial Y^{'}}=4(T^{'}-T_0^{'})I^{'};\ I^{'}=\int_0^{\infty}K_{\lambda\omega}\left(\frac{\partial e_{b\lambda}}{\partial T^{'}}\right)d\lambda, \tag{4}$$

where $K_{\lambda\omega}$ is the absorption coefficient at the wall and $e_{b\lambda}$ is the Plank constant. Here we assume that the temperature differences within the flow are sufficiently small.

The appropriate boundary conditions for the velocity, temperature and concentration fields are given as follows:

$$U^{'}=0,\qquad \frac{dT^{'}}{dY^{'}}=0,\ \frac{dC^{'}}{dY^{'}}=0\qquad at\,Y^{'}=0.$$

$$\mu\frac{dU^{'}}{dY^{'}}=0\quad T^{'}=T_1^{'},\quad C^{'}=C_1^{'}\qquad at\,Y^{'}=H \tag{5}$$

3. Method of solution

Introducing the following non-dimensional quantities:

$$\begin{aligned}
&X^{'}=a\,x,\ \ Y^{'}=a\,y,\ \ H=a\,h,\ \ U^{'}=\frac{\mu u}{\rho a^2},\ \ P=\frac{\mu^2p}{\rho a^2},\ \ \eta=\alpha^2+M,\ \ \mathrm{Pr}=\frac{\mu Cp}{\kappa},\ \ \alpha^2=\frac{a^2}{K^{'}},\\
&Br=\frac{\mu^3}{\rho^2a^4\kappa\left(T_1-T_0\right)},\ C^{'}=C_0+\left(C_1-C_0\right)C,\ -\frac{\partial P}{\partial x^{'}}=\frac{\mu^2L_1}{\rho a^3}\left(L_1=-\frac{\partial p}{\partial x}\right),\\
&\phi=S+N,M=\frac{\sigma B_0^2\,a^2}{\mu},\ Gc=\frac{g\beta\left(C_1-C_0\right)a^4}{\upsilon^2},\ \ S=\frac{S^{'}}{U^{'}\rho Cp},\ N=\frac{16a\sigma^{'}\left(T_1^{'}-T_0^{'}\right)T_0^{'3}}{U^{'}\rho Cp},\\
&T^{'}=T_0+\left(T_1-T_0\right)\theta,\quad \frac{\partial T^{'}}{\partial X^{'}}=\frac{\left(T_1-T_0\right)}{a}L_2\left(L_2=\frac{\partial\theta}{\partial x}\right),\quad \gamma=k_l\,a^2,
\end{aligned} \tag{6}$$

Using (6), the governing equations (1)-(4) are reduced in non-dimensional form as follows:

$$\frac{d^2u}{dy^2}-\eta u=-L_1-Gc\,C, \tag{7}$$

$$\frac{d^2\theta}{dy^2}=\mathrm{Pr}\,a\,L_2\,u-Br\left(\frac{du}{dy}\right)^2-Br\,M\,u^2+S\,\theta+N\,\theta, \tag{8}$$

$$\frac{d^2C}{dy^2} - \gamma C = 0, \tag{9}$$

The corresponding boundary conditions are reduced as:

$$u = 0, \qquad \frac{d\theta}{dy} = 0, \quad \frac{dC}{dy} = 0 \qquad at\ y = 0,$$

$$\frac{du}{dy} = 0, \quad \theta = 1, \quad C = 1 \qquad at\ y = h \tag{10}$$

On solving the above differential equations (7)-(9) under the boundary conditions (10), the exact solutions are obtained for the velocity, temperature and concentration distribution. These expressions are given in eqution (11), (12) and (13). We have formed now forming the following significant features of the flow:

$$u = B_6 e^{\sqrt{\eta}\,y} + B_5 e^{-\sqrt{\eta}\,y} + \frac{L_1}{\eta} - B_1 e^{\gamma y} - B_1 e^{-\gamma y}, \tag{11}$$

$$\theta = R_{28} e^{\sqrt{\phi}\,y} + R_{29} e^{-\sqrt{\phi}\,y} + R_1 e^{\sqrt{\eta}\,y} + R_2 e^{-\sqrt{\eta}\,y} - R_4 e^{\gamma y} - R_4 e^{-\gamma y} + R_{19} - R_{20} e^{2\sqrt{\eta}\,y} - R_{21} e^{-2\sqrt{\eta}\,y} + R_{22} e^{2\gamma y} + R_{23} e^{-2\gamma y}, \tag{12}$$

$$C = A_2 e^{\gamma y} + A_2 e^{-\gamma y}, \tag{13}$$

The flow rate:

$$\psi = \int_0^h u\,dy = \left[\frac{B_6 e^{\sqrt{\eta}\,h}}{\sqrt{\eta}} - \frac{B_5 e^{-\sqrt{\eta}\,h}}{\sqrt{\eta}} + \frac{L_1}{\eta} h - \frac{B_1 e^{\gamma h}}{\gamma} + \frac{B_1 e^{-\gamma h}}{\gamma} - B_7 \right] \tag{14}$$

The mean velocity:

$$\bar{u} = \frac{1}{h}\int_0^h u\,dy = \frac{1}{h}\left[\begin{array}{l} \frac{B_6 e^{\sqrt{\eta}\,h}}{\sqrt{\eta}} - \frac{B_5 e^{-\sqrt{\eta}\,h}}{\sqrt{\eta}} + \frac{L_1}{\eta} h - \frac{B_1 e^{\gamma h}}{\gamma} \\ + \frac{B_1 e^{-\gamma h}}{\gamma} - B_7 \end{array} \right] \tag{15}$$

The mean temperature:

$$\bar{\theta} = \frac{1}{h}\int_0^h \theta\,dy = \frac{1}{h}\left[\begin{array}{l} \frac{R_{28} e^{\sqrt{\phi}h}}{\sqrt{\phi}} - \frac{R_{29} e^{-\sqrt{\phi}h}}{\sqrt{\phi}} + \frac{R_1 e^{\sqrt{\eta}h}}{\sqrt{\eta}} - \frac{R_2 e^{-\sqrt{\eta}h}}{\sqrt{\eta}} - \frac{R_4 e^{\gamma h}}{\gamma} + \frac{R_4 e^{-\gamma h}}{\gamma} + R_{19} h - \frac{R_{20} e^{2\sqrt{\eta}h}}{2\sqrt{\eta}} - \frac{R_{21} e^{-2\sqrt{\eta}h}}{2\sqrt{\eta}} \\ + \frac{R_{22} e^{2\gamma h}}{2\gamma} - \frac{R_{23} e^{-2\gamma h}}{2\gamma} - R_{30} \end{array} \right] \tag{16}$$

Mean Concentration:

$$\bar{C} = \frac{1}{h}\int_0^h C\,dy = \frac{1}{h}\left[a_1 \frac{e^{\gamma y}}{\gamma} - a_2 \frac{e^{-\gamma y}}{y} \right] \tag{17}$$

Where A_1 to A_2, B_1 to B_7 and R_1 to R_{30} are the constant and not given due to sake of breavity.

4. Skin-friction coefficient

The non-dimensional shearing stress in terms of coefficient of skin-friction on the free surface$(C_f)_{y=h}$ and insulated bottom walls$(C_f)_{y=0}$ given by the folowing expressions respectively:

$$\left(C_f\right)_h = \left[\frac{\tau_w}{\rho v^2}\right] = \left[\frac{1}{a^3}\left(\frac{\partial u}{\partial y}\right)\right]_{y=h}. \tag{18}$$

$$\left(C_f\right)_{y=0} = \left[\frac{\tau_w}{\rho v^2}\right] = \left[\frac{1}{a^3}\left(\frac{\partial u}{\partial y}\right)\right]_{y=0}. \tag{19}$$

5. Nusselt number

The rate of heat transfer in terms of Nusselt number on the free surface $(Nu)_{y=h}$ and insulated bottom wall $(Nu)_{y=0}$ is given by following expressions respectively

$$\left(Nu\right)_{y=h} = \left[\frac{d\theta}{dy}\right]_{y=h} \tag{20}$$

$$\left(Nu\right)_{y=0} = \left[\frac{d\theta}{dy}\right]_{y=0} \tag{21}$$

6. Sherwood number

The rate of mass transfer in terms of Sherwood number on the free surface $(Sh)_{y=h}$ and insulated bottom wall $(Sh)_{y=0}$ is given by following expressions respectively

$$\left(Sh\right)_{y=h} = \left[\frac{dC}{dy}\right]_{y=h} \tag{22}$$

$$\left(Sh\right)_{y=0} = \left[\frac{dC}{dy}\right]_{y=0} \tag{23}$$

Table:1 The numerical values of skin-friction coefficient, Nusselt number and Sherwood number at the channel for different physical values when a=0.5

S.No	S	Pr	r	H	c	γ	N	M	$(C_f)_{y=0}$	$(C_f)_{y=h}$	$(Nu)_{y=0}$	$(Nu)_{y=h}$	$(Sh)_{y=0}$	$(Sh)_{y=h}$
I	0.5	0.71		.5	3	1	1	1	-	-	-31.5	-35.7	-	-
II	1	0.71		.5	3	1	1	1	-	-	-33.2	-47.5	-	-
III	0.5	7.0		.5	3	1	1	1	-	-	-23.2	-52.39	-	-
IV	0.5	0.71	.5	.5	3	1	1	1	1.64	-0.86	-47.7	-53.62	-	-
V	0.5	0.71			3	1	1	1	1.64	-0.86	-8.80	-14.50	0.33	0.64
VI	0.5	0.71		.5	5	1	1	1	-1.04	-4.00	-59.9	-78.81	0.46	0.886
VII	0.5	0.71		.5	3	3	1	1	2.388	-0.22	1.35	3.2995	2.71	0.425
VIII	0.5	0.71		.5	3	1	2	1	1.15	-2.85	-33.9	-68.22	-	-
IX	0.5	0.71		.5	3	1	1	2	-	-	-26.4	-51.84	-	-

7. Result & Discussion

This study reflects the fluid flow configuration through a horizontal channel soaked with porous medium having fixed impermeable thermally insulated bottom surface. The significant effects of numerous constraints or parameters on the heat and mass transfer in forced convective flow in the presence of heat source and thermal radiation are calculated. In addition of that mean temperature, mean velocity and mean concentration of species are also considered as well. These results are presented through graphs and tables.

The influence of different physical parameters are showed by the figures 2 and 3. Fig.2 represents that due to the high intensity of applied magnetic field and chemical reaction coefficient, the fluid velocity is reduced throughout the channel. But the reverse effect can be seen by increasing the mass buoyancy parameter Gc. It is observed from fig.3 that the fluid velocity is upsurging from the bottom surface to the top free surface with the rise of permeability parameter. When the permeability of any porous medium rises the fluid flow become easier through it, due to the larger void space in porous medium and less resistance in it. This is the basic reason that the fluid velocity is perceived to the zero at the insulated bottom surface and progressively it rises as it extents to the free surface and achieves an extreme value nearby. We can see the effect of depth of the channel on the velocity field by the fig.3. It is clear, as the depth increases; the fluid velocity is upsurging at all the points of the channel in the same porous medium.

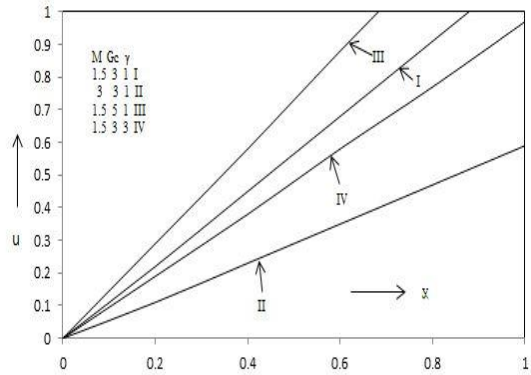

Fig.2. Velocity distribution versus y when h=1.

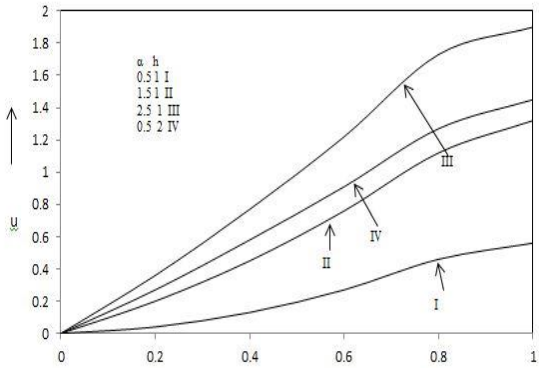

Fig.3. Velocity distribution verus y when M=1.5, Gc=3 and γ=1.

Fig.4 and 5 illustrate that the fluid temperature is rising with the increases of magnetic intensity, Brinkman number, heat source and chemical reaction parameter while adverse behaviour is observed due to the upsurge in Prandtl number, radiation parameter and Grashof number for mass transfer. From fig.6 it is seen that fluid temperature is growing with the increase of porosity parameter while reverse effect is seen in the case of increment of depth size of channel.

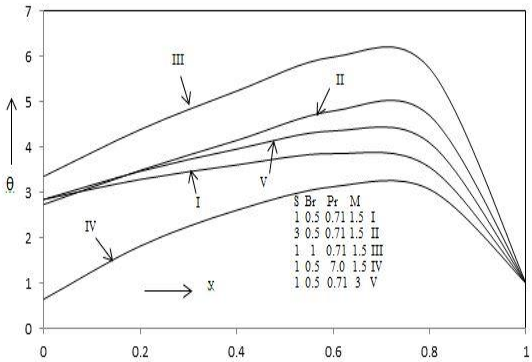

Fig.4. Temperature distribution versus y when h=1, Gc=3, γ=2, N=1.

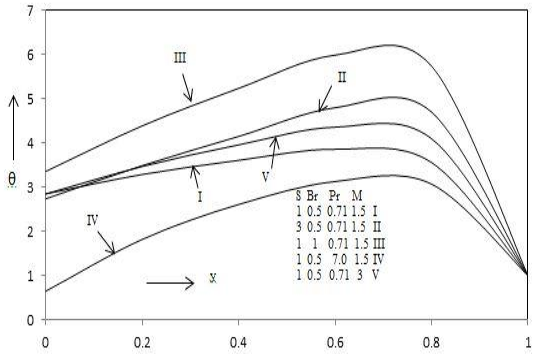

Fig.5. Temperature distribution versus y when h=1, S=1, Br=0.5, M=1.5, Pr=0.71.

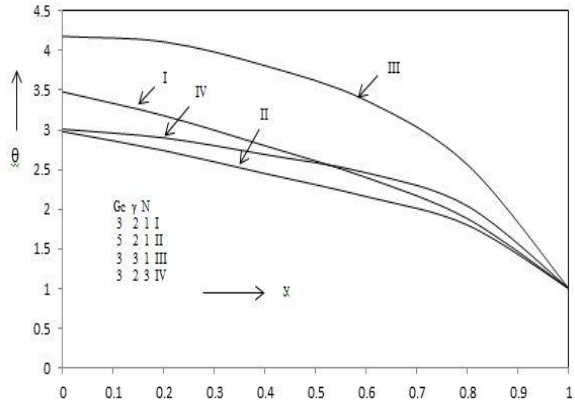

Fig.6. Temperature distribution versus y when Gc=3, S=1, Br=0.5, M=1.5, Pr=0.7, γ=1, N=1.

It is provided from fig.7 that species concentration is declining throughout the fluid flow due to the increase of chemical reaction parameter and depth size.

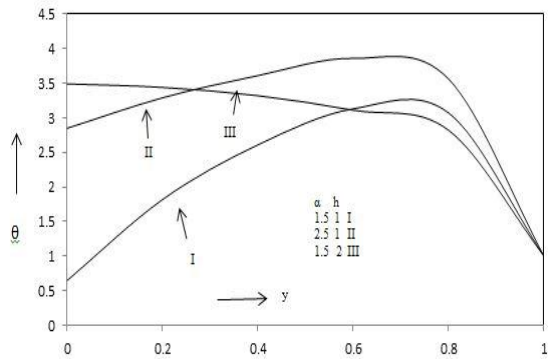

Fig.7. Temperature distribution versus y when Gc=3, S=1, Br=0.5, M=1.5, Pr=0.7, γ=1, N=1.

The effect of various parameters on mean velocity is reflected by fig.8 and 9. It is observed that the mean velocity of the fluid is growing with the intensity of magnetic field, chemical reaction coefficient, permeability parameter, mass buoyancy and depth of channel.

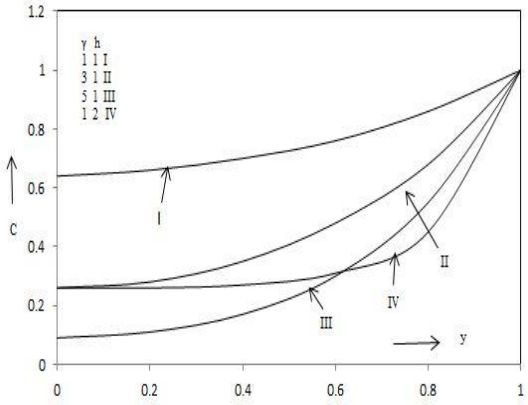

Fig.8. Concentration distribution versus y.

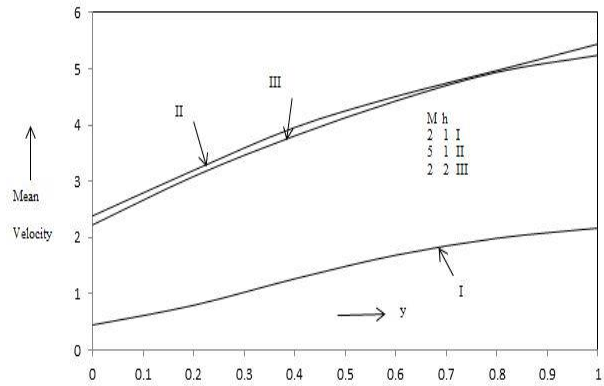

Fig.9. Mean velocity versus y when Gc=3, γ=1, α=0.5

From fig.10 and 11, it is clear that the mean temperature rises with the increase of heat source, Brinkman number, radiation parameter, chemical reaction coefficient, Prandtl number and mass buoyancy; while the reverse effect is observed due to increase in intensity of magnetic field. Fig.12 shows that when we increase the depth of open channel the value of the mean temperature of the fluid flow become high at insulated bottom wall and then reduced gradually when approaches to open surface. Adverse behaviour is observed in the case of permeability parameter.

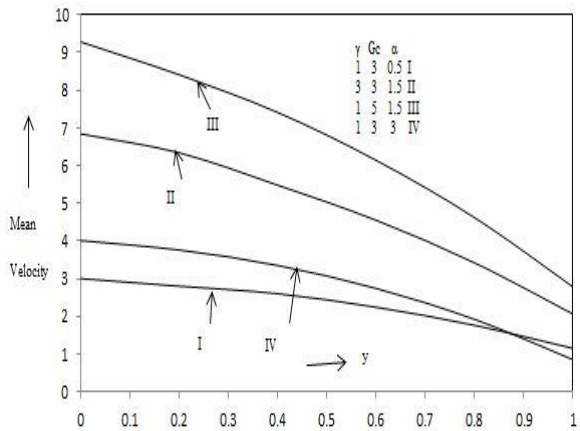

Fig.10 Mean velocity versus y when h=1, M=0.5.

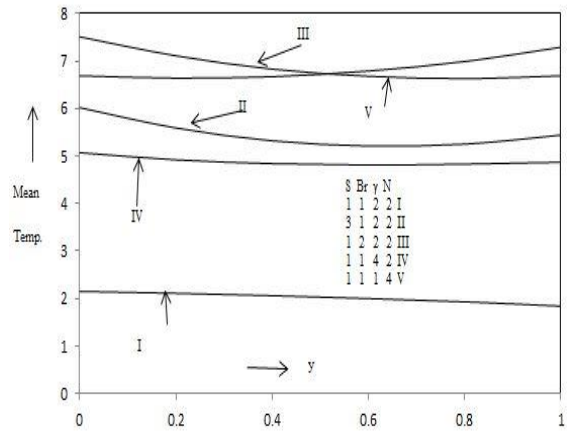

Fig.11. Mean temperature versus y when Gc=3, γ=1, α=0.5, Pr=0.71, M=0.5, h=1.

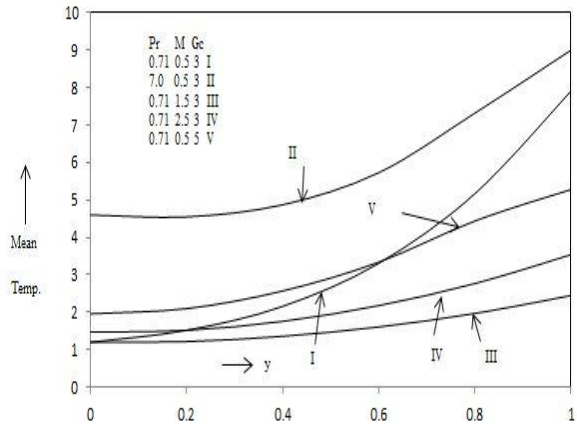

Fig.12. Mean temperature versus y when S=0.5, Br=1, N=1, γ=1, α=0.5, h=1.

Fig.13 shows that the mean concentration is upsurging with the rising values of chemical reaction coefficient and depth of the open channel.

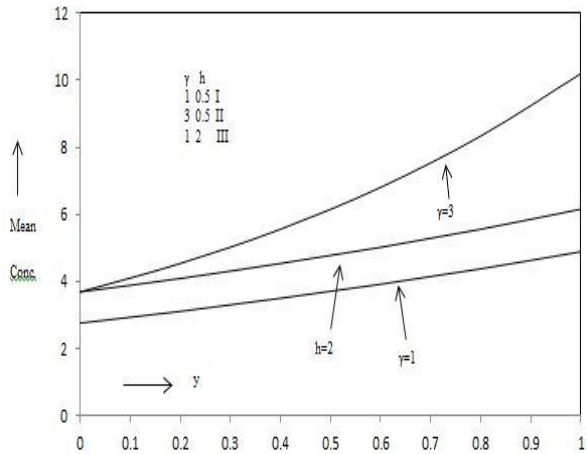

Fig.13. Mean concentration versus y.

Table1 depicts the values of skin-friction coefficient, Nusselt number and Sherwood number at insulated bottom surface as well as free top surface. At insulated bottom surface the value of skin-friction coefficient is increasing with the upsurging values of mass buoyancy. While it is decreasing with the increase of Grashof number of mass transfer. The same behaviour is observed for skin-friction coefficient at free surface.

At insulated bottom wall the value of Nusselt number is growing up with the increase in depth of the channel, chemical reaction coefficient and Prandtl number, while it is reducing with the increment in the values of heat source parameter, Brinkman number, mass buoyancy and radiation parameter. Nusselt number at free surface is rising with the upsurged values of chemical reaction parameter and depth of the channel, whereas declining with the increase values of heat source, Prandtl number, Brinkman number, mass buoyancy and radiation parameter. It is seen through the table-1 at insulated bottom surface, the Sherwood number is escalating with the raised values of chemical reaction coefficient but it is decreasing with the increase value of open channel. At free surface, Sherwood number is declining with the upsurge values of chemical reaction coefficient and channel depth.

8. Conclusion

In the present study we considered a horizontal channel in which, bottom surface is made with insulated material while top surface is free surface. We deliberated the steady flow of viscous fluid of fixed depth through a porous medium under forced convection and transverse magnetic field. The flow is created by a constant horizontal pressure gradient parallel to the insulated fixed bottom surface. A theoretical study has been covered by the effects of various parameters considered in the flow problem. The following conclusions are made by the obtained results:

(1) Velocity and mean velocity of the fluid is increasing from the insulated bottom surface to the free surface with the increment in porosity parameter α. Since, when the permeability of the medium increases then the resistance of the medium becomes stumpy; therefore the fluid may flow easily through it. This is the reason that the velocity at insulated surface at bottom level is seen to be zero and then it takes its maximum value at top free surface.

(2) Velocity and mean velocity of the fluid show there positive behaviour with the increase in mass buoyancy and depth of the porous medium. Both are in increasing order with these parameters. In the case of large values of depth of porous medium the velocity and mean velocity attain its high values throughout the fluid flow. This is concluded that by increasing the depth of porous medium; the fluid flow can be made fast in this

geometrical fluid flow. This study has been done in the presence of transverse magnetic field and chemical reaction coefficient.

(3) Mean velocity shows its good approach in the presence of chemical reaction effect. Due to its presence mean velocity attains its high values at insulated bottom wall, but it is getting reduce rapidly when it approaches to free surface.

(4) By using the effects of chemical reaction and external heat source; the temperature and mean temperature both can be extended for their high values. In the case of mean temperature; it shows its positive behaviour with respect to the radiation coefficient and intensity of the transfer magnetic field.

(5) For high depth porous medium channel, the fluid mean temperature and species mean concentration both rise high.

(6) By increasing in the values of porosity parameter; the mean temperature of the fluid decreases. This is because of the existence of joule heating which diminishes the temperature due to the free expansion.

References

1. Y. Kuznestov, L. Levitin, E.P. Markov, D.L. Orlov, O. N. Popov, Effect of thermal insulation of the bottom of a melting tank on mass exchange of the glass, 1986, Glass Ceram, vol. 43, pp. 238-241.
2. F.A. Abdullah, Theoretical and experimental investigation of natural composite materials as thermal insulation, 2011, Al-Qadisiya J. Eng. Sci., vol. 4, pp. 26-36.
3. A.N. Reddy, N.S.V.K. Verma and M.C. Raju, Thermo diffusion and chemical effects with simultaneous thermal and mass diffusion in MHD mixed convection flow with ohmic heating, 2009, J. Naval Architect Mar. Eng., vol. 6, pp. 84-93.
4. S. Yao, L. Lei, J. Deng, S. Lu, W. Zhang, Heat transfer mechanism in porous copper foam wick heat pipes using nanofluids, 2015, Int. J. of Heat & Tech, vol. 33, no. 3, pp. 133-138.
5. F. Zeng, C. Long and J. Guo, Research on heat transfer and three dimensional characteristic of natural convection in a small cavity with heat source, 2015, Int. J. of Heat & Tech, vol. 33, no. 3, pp. 59-66.
6. I.G. Baoku, B.I. Olajuwon, A.O. Mustapha, Heat and mass transfer on a MHD third grade fluid with partial slip flow past an infinite vertical insulated porous plate in a porous medium, 2013, Int. J. of Heat and Fluid Flow, vol. 40, pp. 81-88.

7. P.M. Thakur and G.C. Hazarika, Effects of variable viscosity and thermal conductivity on the MHD flow of micropolar fluid past an accelerated infinite vertical insulated plate, 2015, Int. J. of Heat & Tech, vol. 33, no. 3, pp. 73-78.
8. B.K. Jha, B. Aina and A.T. Ajiya, MHD natural convection flow in a vertical parallel plate microchannel, 2015, Ain Shams Eng. J., vol. 6, pp. 289-295.
9. J.C. Umavathi, A.J. Chamkha, A. Mateen and A. Al-Mudhal, Unsteady oscillatory flow and heat transfer in a horizontal composite porous medium channel, 2009, Modelling and Control, vol. 14, pp: 397-415.
10. M. Bakkas, A. Amahmid, and M. Hasnaoui, Numerical study of natural convection heat transfer in a horizontal channel provide with rectangular blocks releasing uniform heat flux and mounted on its lower wall, 2008, Energy Conversion and Management, vol. 49, pp. 2757-2766.
11. Z. Ma, L. Duan, S. Yao and X. Jia, Numerical study of natural convection heat transfer in porous media square cavity with multiple cold walls based on LBM, 2015, Int. J. of Heat & Tech, vol. 33, no. 4, pp. 69-76.
12. S. Pravin and N.F. Hossain, Investigation on the conjugate effect of joule heating and magnetic field in combined convection in a lid driven cavity with undulated bottom surface, 2010, J. Advan. Sci. Eng. Res., vol. 1, pp. 210-223.
13. C. Liu W. and C. Gau, Onset of secondary flow and enhancement of heat transfer in horizontal convergent and divergent channels heated from below, Int. J. Heat Mass Trans., Vol. 47, pp: 5427-5438.
14. O.D. Makinde and P.Y. Mhone, On temporal stability analysis for hydromagnetic flow in a channel filled with a saturated porous medium flow, 2009, Turbul Combust, vol. 83, pp. 21-32.
15. K. Mounuddin, N.C.H. Pattabhiramacharyulu, Steady flow of a viscous fluid through a saturated porous medium of finite thickness impermeable and thermally insulated bottom and the other side is stress free at a constant temperature, 2010, J. Pure Appl. Phys, vol. 22, pp. 107-122.
16. K.V.S. Raju, T.S. Reddy, M.C. Raju, P.V.S. Narayana, S. Venkataramana, MHD convective flow through porous medium in a horizontal channel with insulated and impermeable bottom wall in the presence of viscous dissipation and joule heating, 2014, Ain Shams Eng. J., vol. 5, pp. 543-551.
17. I. Zeghbid, R. Bessaih, Mixed convection in Lid-Driven cavities filled with nanofluid, 2015, Int. J. of Heat & Tech, vol. 33, no. 4, pp. 77-84.

18. S.E. Rafiee, M.M. Sadeghiazad, Heat and mass transfer between cold and hot vortex cores inside Ranque-Hilsch vortex tube optimization of heat tube length, 2016, Int. J. of Heat & Tech, vol. 34, no. 1, pp. 31-38.
19. H.B. Niche, S. Bouabdallah, B. Ghernaout, M. Teggar, Unsteady double diffusive natural convection with doufour and soret effects, 2016, Int. J. of Heat & Tech, vol. 34, no. 1, pp. 39-46.
20. A.O. Popoola, I.G. Baoku, B.I. Olajuwan, Heat and mass transfer on MHD viscoelastic fluid flow in the presence of thermal diffusion and chemical reaction, 2016, Int. J. of Heat & Tech, vol. 34, no. 1, pp. 15-26.
21. N. Ahmed, S.M. Das, Oscillatory MHD mass transfer channel flow in a rotating system with hall current, 2016, vol. 34, no. 1, pp. 115-123.
22. K. Yamamoto, N. Iwamura, Flow through a porous wall with convection acceleration, 1974, J. Phys. Soc. Jpn, vol. 37, pp. 774-779.
23. A.C.L. Cogley, W.G. Vinvent, and E.S. Giles, Differential approximation for radiative heat transfer in non-linear equations-grey gas near equilibrium, 1968, American Institute of Aeronautics, vol. 6, pp. 551-553.

Nomenclature

u	Non-dimensional velocity along the x-axis	K_l	Chemical reaction parameter
K’	Dimensional porous parameter	Pr	Prandtl number
U'	Velocity of the fluid along X’-axis	Nu	Nusselt number
g	Acceleration due to gravity	Gc	Grashof number for mass transfer
Sh	Sherwood number	H	Depth of the porous medium along Y’-axix
B_0	Strength of uniform magnetic field	S	Heat source parmeter
C	Non-dimensional of concentration of species	Br	Brinkman number
N	Radiation parameter	H	Sum of magnetic parameter and permeability
a	Some standard length	$\bar{\theta}$	Mean Temperature
T_0	Temperature of the upper open surface	K	Thermal conductivity

T'	Temperature of the fluid	A	Permeability parameter in the dimensionless form
T_1	Temperature at the bottom surface	M	Kinematic viscosity
Cp	Specific heat at constant pressure	β	Volumetric coefficient of expansion with species concentration
C_0	Species concentration at the upper open surface	σ	Electrical conductivity
C_1	Species concentration at the bottom surface	P	Density of the fluid
$\bar{u}$	Mean velocity	γ	Chemical reaction coefficient
$\bar{C}$	Mean Concentration	θ	Dimensionless temperature of the fluid
P	Pressure of the fluid	M	Hartmann number
C_f	Skin-friction coefficient		